

# Variation of monthly exploitable wave energy in the Gulf of Chabahar under a high-resolution CMIP6

Mahmoud Pourali<sup>1\*</sup>, Mohamad Reza Kavianpour<sup>2</sup>

<sup>1</sup> Faculty of Civil Engineering, K.N. Toosi University of Technology; [m.pourali@email.kntu.ac.ir](mailto:m.pourali@email.kntu.ac.ir)

<sup>2</sup> Faculty of Civil Engineering, K.N. Toosi University of Technology; [kavianpour@kntu.ac.ir](mailto:kavianpour@kntu.ac.ir)

## ARTICLE INFO

### Article History:

Received: 28 Oct. 2022

Accepted: 11 Dec. 2022

### Keywords:

Wave energy

Climate change

Weibull-based bias-correction

Gulf of Chabahar

Emission scenario

## ABSTRACT

Electric energy consumption is growing almost all over the world. Similarly, using clean resources in coastal such as wave power is also growing. The coasts of Oman Gulf in southeast of Iran is one of the most potential areas for deriving energy from waves. The sea waves are mostly generated by wind and the climate change affect the wind field. Hence evaluating climate change effects on the wave power is essential for energy extraction. In this research, the variation of monthly average in Chabahar bay wave power under the middle scenario of future climate effect has been studied. For this, the CNRM-CM6-SSP2-45 dataset has been downscaled with the Weibull technique, and with a calibrated wave model, wave characteristic has been calculated. Based on the results, the average annual wave power will reach 10.4 kW/m by an increase of 3%. Total wave energy in Chabahar is about 91,000 kWh/m during the year, which will also increase by 3% compared to the same period previous century. In the July and August, the first high energetic months, the wave power increase by 1% on average compared to the previous period. The highest monthly increase occurs in October and with a 277% increase, it reaches 5535 kW/m. The highest monthly decrease of 25% occurs in June and the energy reaches from 13041 to 9513 kW/m.

## 1. Introduction

As a renewable resource, wave energy represents one of the cleanest sources of energy. There has been an increase in the use of this type of energy in coastal regions over the past two decades. In the regions with higher significant wave heights and longer periods, wave energy can be considered a primary alternative to fossil fuels. In this regard, Chabahar bay, located in the coasts of the Gulf of Oman, has great potential over all the Iranian seas. Several factors in this region, including higher waves, continuity of the long waves, specifically in the summer, and synchronicity of these waves with peak hours of energy consumption in the area, verify the suitability of this area for using the waves as an energy resource. Another crucial factor is the cost of converting fossil fuels to electricity. Generally, in the process of producing electric energy, fossil fuels are transported to a location near the place of use, where they will be transformed into electric energy using fossil power plants. Hence, in areas such as Chabahar in Sistan and Baluchestan province which are far from fossil fuel sources, the final cost of electric energy driven from the fuel is higher than its cost in regions located near fossil energy sources.

Selecting the location of installation for energy exploitation devices, known as Wave Energy Converter (WEC), is extremely important [1]. The type of device, depth of installation, and amount of achieved energy are related and selected concerning each other. Regions with higher wave heights and periods possess more energy. The wave energy variation due to changing characteristics of the wave components in different seasons is inevitable. Generally, regions with more energy stability are better for energy exploitation [2]. Another crucial factor is the climate change impact on waves energy amount. Therefore, several studies were conducted on wave energy variation due to climate change [3–7].

Global Circulation Models (GCM) are large-scale meteorology models which simulate effective atmospheric variables on the climate in future conditions. These models are based on different scenarios and cannot be used in local-scale models regarding their large scales. Based on the most recent update from Intergovernmental Panel on Climate Change (IPCC) for Coupled Model Intercomparison Project Phase (CMIP6), climate variables under different Shared Socioeconomic Pathways (SSP) have

been presented. Since these results are global and large-scale, they need to be downscaled for use in local models.

Martinez and Iglesias [8,9] investigated the wind resources under different climates and CMIP6 scenarios in Europe and Northern America. While wave variables, such as height, period, etc., are not presented in GCM models directly. Since the waves are created by wind, an intermediate wave model is needed to calculate the wave properties using the wind field. As a result, a numerical model is developed in which the wind velocity components in two axes of x and y (or wind speed and direction), are used as the force that creates waves.

Due to its large scale, GSM data should be downscaled. Wind downscaling previously relied on statistical or dynamic downscaling. Regression models, artificial intelligence, and Weibull distributions are some of the known statistical downscaling techniques, while applying numerical models such as WRF for downscaling is known as a dynamic technique. Weibull's method does not modify the order or sequence of occurrences, which is crucial for wave simulation. The primary Weibull method, which was presented in a summative format, was modified with the knowledge that this equation is naturally multiplicative due to the presence of two form factors [10]. It results in better statistical values compared to those of the common Weibull method. This research utilized the modified Weibull method.

Swell waves from the south of the Indian Ocean reach the Gulf of Oman and the Gulf of Chabahar. The study area in this research is exposed to waves created by the Monsoon winds. As for Chabahar Bay, a safe area was established for landing buoyant, which resulted in resident accumulation and human concentration. According to the listed characteristics, this area has a high potential for energy exploitation. Wave energy in this zone has been studied before in some research [11,12]. These studies were based on the average energy of waves. In [13], a multi-factor procedure has been presented for selecting a combination of WECs and alternative situations in the Caspian Sea, Persian Gulf, and the Gulf of Oman. The noted research considered several factors, including exploitable energy, availability, total obtained energy, and inter-seasonal changes.

One of the main steps for obtaining a reliable result is providing a calibrated numerical model in the study area. Therefore, the wave simulation was conducted using a third-generation DHI MIKE 21 Spectral Wave model [14]. This model calculates wind generated wave characteristics such as height, period, direction, and energy.

In this study, CNRM wind data has been modified with reliable ERA5 wind data. Correction has been based on correction coefficients that has been obtained in past period. For this a modified version of Weibull

downscaling has been used. Then, wave simulation was done using the new modified CNRM wind field in past and future periods, and the wave energy was extracted and compared from the results of the wave model.

The data and the selected method are explained in section 2. A summary of the results of this study is presented in Section 3. The conclusion of the study is discussed in section 4.

## 2. Data and selected method

The general procedure of this research is as follows:

- Selecting the study area
- Collecting data from the considered dataset
- Modifying (downscaling) the wind field
- Investigating the obtained wind field
- Providing the calibrated wave model
- Waves modeling (past and future periods)
- Extracting the wave energy
- Processing and examining the wave power changes

The wave energy is calculated using the MIKE21 SW numerical model. It is based on the third generation of wave equilibrium equations. MIKE21 SW uses a spectral action balance equation considering the growth, decay and transformation of wind-generated waves and swells in offshore and coastal areas. It means that calculates the wind generated wave parameters in each timestep. Therefore, climate change is visible in the studied waves indirectly using downscaled wind field.

### 2.1. Study area

The study area is the coastal region of the Gulf of Chabahar in the southeast of Iran's coasts in the Gulf of Oman, which has a great potential for wave energy. The measurements in two points near this location were used to calibrate the wave model. The results of the model in these points were investigated to verify their accuracy. Then the wave energy was investigated at a point with 29 meters depth off the coast of Chabahar Bay. Table 1 and Figure 1 show the locations of the points used in modeling and investigating the wave energy.

**Table 1. Location of the wave model calibration**

Station	Longitude (deg)	Latitude (deg)	Depth (m)	Use
Jask	57.753	25.608	25	Calibration
Chabahar	60.5	25.267	17	Calibration
Energy St.	60.544	25.242	29	Energy Analyze

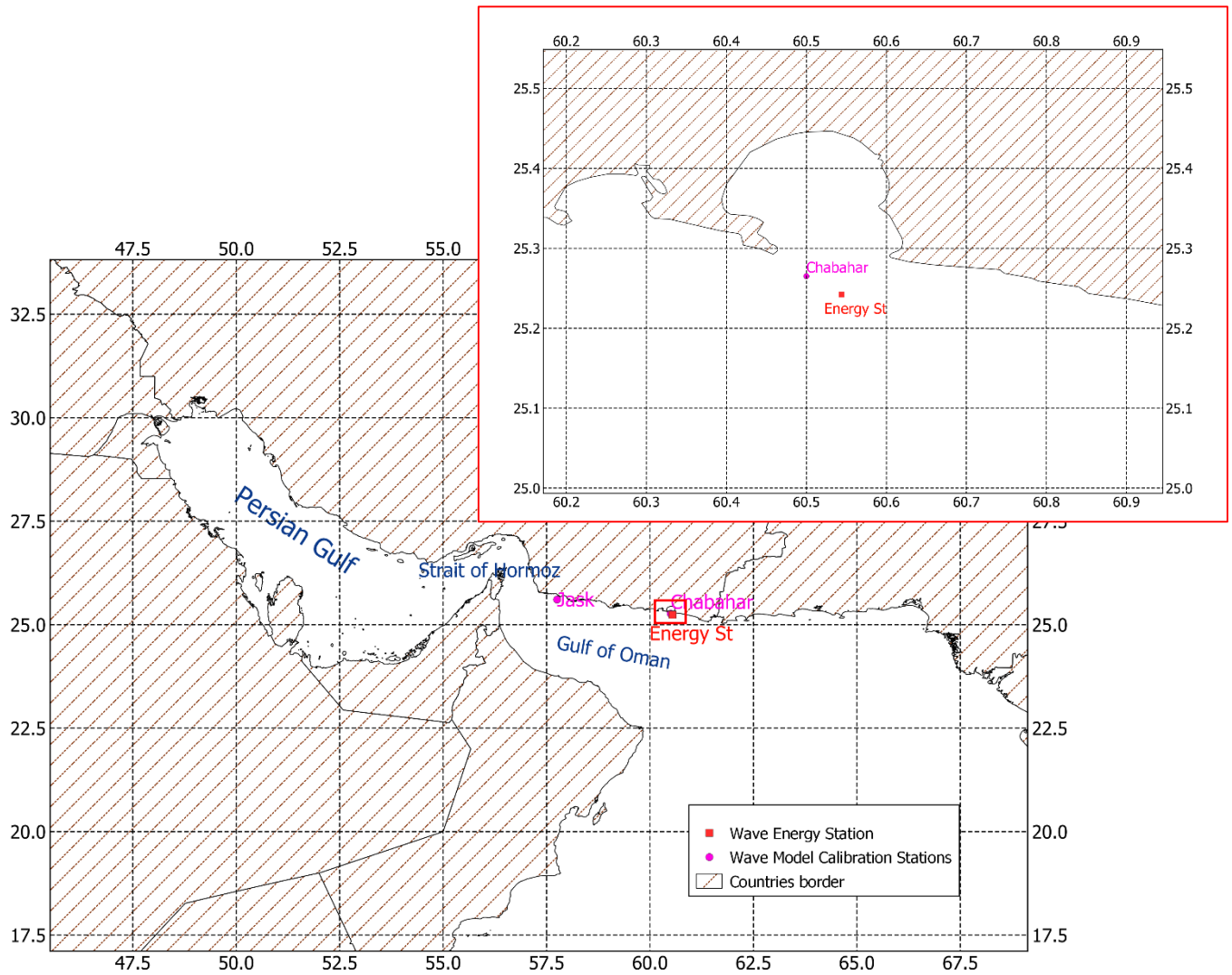


Figure 1. Location of the selected point of the wave model

## 2.2. The wind data

In this study, data from the CNRM-CM6-SSP2-45 dataset of CMIP6 was used. The dataset is available at <https://esgf-data.dkrz.de/search/cmip5-dkrz/>. In addition to good congruence with the measured wind data, this dataset has a higher resolution compared to other GCMs. It is related to an intermediate scenario, which means that it calculates metrology parameters in the future with an average amount of Carbon. So, it is not optimistic or pessimistic. As part of the general purpose of this study, which is to investigate long-term variations in energy levels, waves were examined over two 10-year periods with a difference of 100 years in the past and the future. These periods included 1991 to 2000 as the past period and 2091 to 2100 as the future period.

The time resolution of the 3-hour and their spatial resolution of  $0.5 \times 0.4993$  degree of wind data is available in both the past and the future. Using the improved Weibull method, these data were modified, analyzed, and downscaled. ERA5 data from the reanalysis model were used for this purpose. As a result of previous experience, ERA5 data are in good agreement with measured data. The wind field was

therefore modified using this data as the reference. Based on data from 1991 to 2000 years, wind modification was performed.

## 2.3. Methodology

To improve the asymmetry of data in this study, the improved Weibull method was applied to the wind field. There was a primary version of this technique suggested in [15], and an improved version was proposed in [10]. In general, the Weibull method is as equation 1:

$$f(w) = \frac{k}{A} \left(\frac{W}{A}\right)^{k-1} \exp\left[-\left(\frac{W}{A}\right)^k\right] \quad (1)$$

Where  $W$  is the wind speed, and  $A$  and  $k$  are the coefficients of scale and shape in the Weibull distribution, respectively. Therefore, they are calculated based on the reference data (ERA5) using 2 and 3 equations and are applied using equations 4 and 5 to the CNRM wind data.

$$D_{A(i)} = \frac{A_{ERA5(i)}^{His}}{A_{CNRM(i)}^{His}} \quad (2)$$

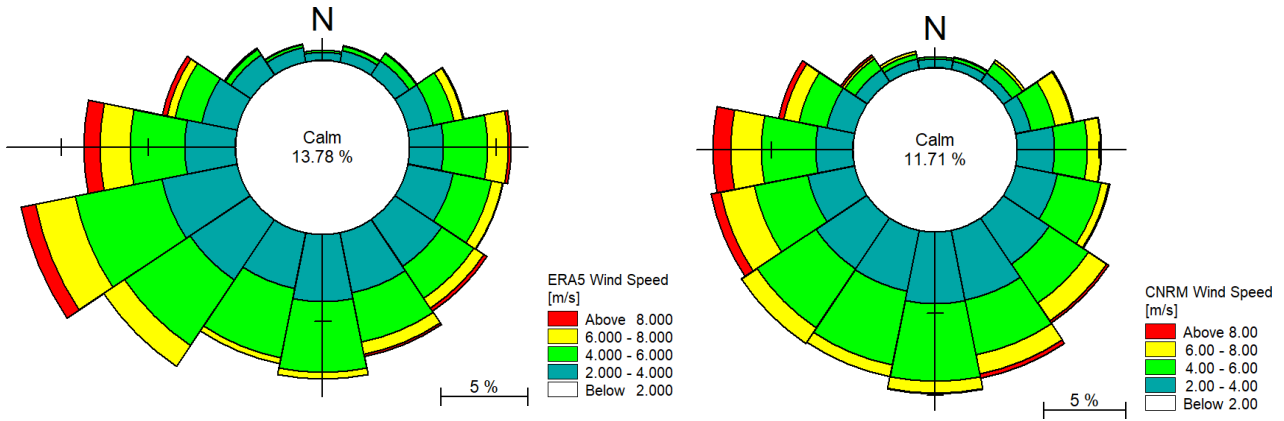


Figure 2. The modified wind rose of CNRM through the modified Weibull method (right), and the reference wind rose of ERA5 (left)

$$D_{k(i)} = \frac{k_{ERA5(i)}^{His}}{k_{CNRM(i)}^{His}} \quad (3)$$

$$A_{CNRM(i)}^{Future} = A_{CNRM(i)}^{Future} \times D_{A(i)} \quad (4)$$

$$k_{CNRM(i)}^{Future} = k_{CNRM(i)}^{Future} \times D_{k(i)} \quad (5)$$

In this research, a preprocess was done on the wind dataset. For this, first of all the values of  $D_A$  and  $D_k$  has been obtained based on the modified Weibull method. This process has been done on a two-dimensional matrix on wind datasets. These values are based on modified Weibull technique on both ERA5 and CNRM data and compared to each other. In the next step, both past and future datasets of the CNRM collection were modified using the obtained coefficients. It should be mentioned that these datasets have different spatial resolution. for intermediate points, interpolation should also be used. After modifying the wind dataset, the obtained CNRM wind dataset is applied to a calibrated wave model. In the next step, the values the wave power are extracted from the wave model in both past and future period. In the next step, according to the amount of wave power and the duration of these waves, the energy of the wave is calculated and statistical analyzes were performed on the results. A sample of the modified wind rose is shown in Figure 2. This wind rose is related to the entrance of the Chabahar Bay in the sea.

### 3. Results

#### 3.1. The wave height

In this research MIKE 21 SW has been used for the wave simulation. MIKE 21 SW, a third-generation Spectral Wave model solves the equations on an irregular triangular mesh and simulates hydrodynamics phenomena, both near shore and offshore. Equation 6 shows the principal equation.

$$\frac{\partial N}{\partial t} + \frac{\partial}{\partial \phi} C_\phi N + \frac{\partial}{\partial \lambda} C_\lambda N + \frac{\partial}{\partial \sigma} C_\sigma N + \frac{\partial}{\partial \theta} C_\theta N = \frac{S}{\sigma} \quad (6)$$

Where  $N$  is action density,  $t$  is the time,  $\lambda$  and  $\phi$  are longitude and latitude, respectively,  $\sigma$  is frequency,  $C$  is the wave speed, and  $\theta$  is the wave direction. To simulate waves, a computational triangular irregular mesh with different elements sizes was provided. Figure 3 illustrates the computational mesh and depths in the simulation domain. The computational domain is within the range of 47.8 to 74 (degrees) longitude and 15 to 30.4 (degrees) latitude.

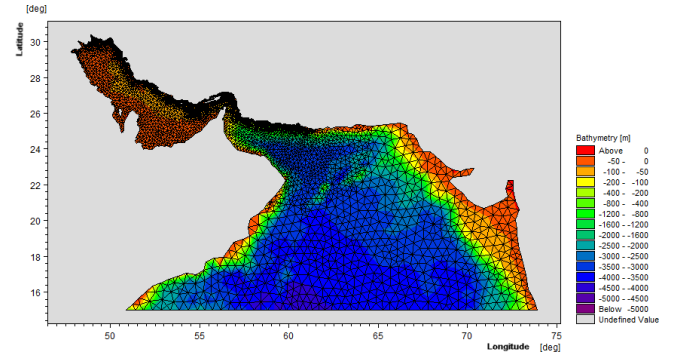


Figure 3. Computational domain and bathymetry the wave simulation

For calibration, the results of the wave model in Jask and Chabahar are compared to the measured values. For this purpose, the simulation has been repeated with different values. Ultimately, values of 2, 0.5, and 0.001 were selected for  $C_d$ , delta in the white capping equation, and Nikuradse's bed roughness coefficient respectively. Figure 4 demonstrates the time series of the results in the Jask and Chabahar stations. For the evaluation of accuracy of the results of the calibrated model, statistical parameters were calculated concerning the measured data. The applied statistical relationships are as equations 7 to 10. Statistical values for the wave model results are presented in Table 2.

$$SI = \frac{\sqrt{\frac{1}{n} \sum (X_p - X_m)^2}}{\bar{X}_m} \quad (7)$$

$$CC = \frac{\sum (X_p - \bar{X}_p)(X_m - \bar{X}_m)}{\sqrt{\sum (X_p - \bar{X}_p)^2 \sum (X_m - \bar{X}_m)^2}} \quad (8)$$

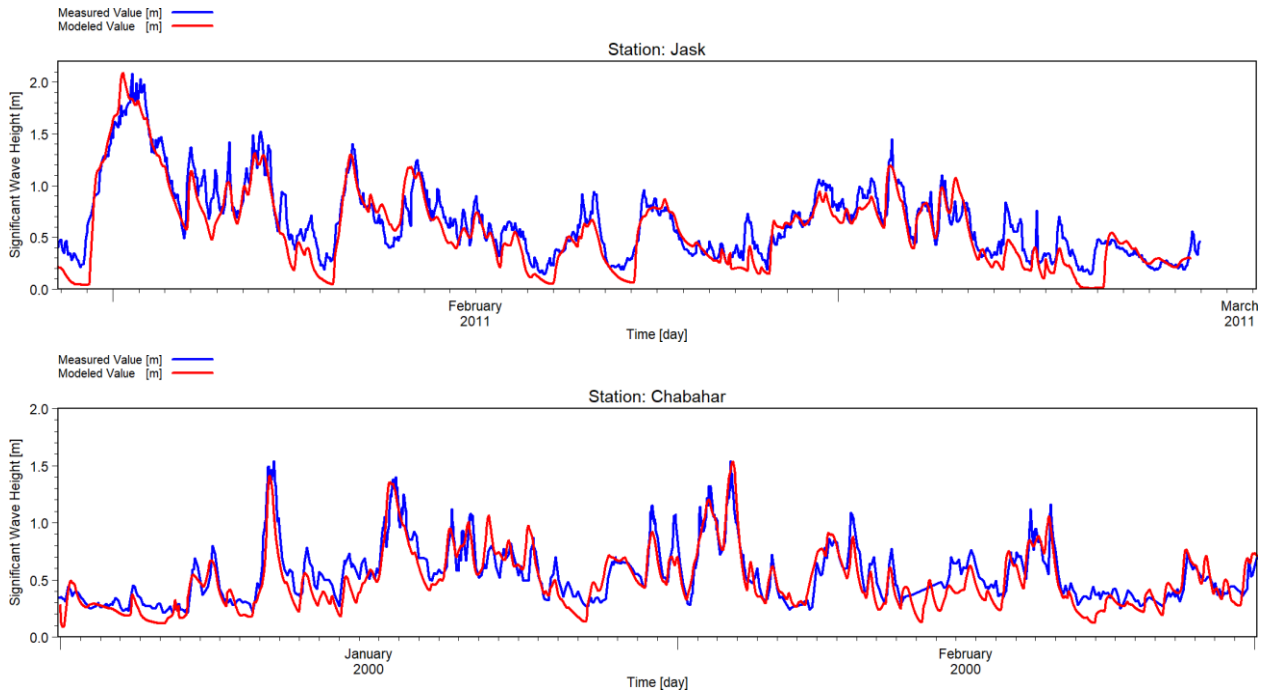


Figure 4. Time series of the simulated and measured wave heights in Jask and Chabahar stations

$$BIAS = \sum \frac{1}{n} (X_p - X_m) \quad (9)$$

$$RMSE = \sqrt{\frac{1}{n} (X_p - X_m)^2} \quad (10)$$

Table 2- Statistical evaluation of simulated waves

Buoy	Jask		Chabahr	
	Feb & Mar 2011	Jan & Feb 2000	Jan & Feb 2000	Jan & Feb 2000
Period	Feb & Mar 2011	Jan & Feb 2000	Jan & Feb 2000	Jan & Feb 2000
Parameter	Hs (m)	Tp (s)	Hs (m)	Tp (s)
SI	0.33	0.16	0.21	0.1
CC	0.83	0.76	0.91	0.92
BIAS	-0.08	-0.03	-0.04	0.02
RMSE	0.19	0.74	0.14	0.12

Based on the obtained statistical results, the prepared wave model is reliable and its results can be used for further analysis.

Figure 5 shows the average significant wave height in the past and future period. The colored palettes are the same for both periods. Based on the results, the significant wave height value has increased slightly.

### 3.2. The wave power and energy

The wave power measured in kW/m is based on the values of the significant wave height and the period, as equation 11 [15,16].

$$P \approx 0.49H_s^2T_e \quad (11)$$

Where  $H_s$  is the significant wave height and  $t_e$  is the energy period.

Considering the durations and wave power, the value of  $P_{ave}$  can be calculated. Also, with  $t$  as the total time per year, the exploitable energy can be calculated.

$$E_t = P_{ave} \times t \quad (12)$$

$$E_e = P_{ave} \times t_e \quad (13)$$

Where  $t$  and  $t_e$  are the total hours and the hours in which the wave energy is larger than a specific value, according to which the exploitable value through WEC specification. In this research, the value of the threshold is considered 2 kW/m. The ratio between  $E_e$  and  $E_t$  is defined as exploitability.

$$Exploitability (\%) = \frac{E_e}{E_t} \quad (14)$$

Figure 6 shows the average wave power in the past and the future. Based on Figure 6, the difference in the average wave power in these two periods is not remarkable. It was found that the mean annual wave energy increased a little. This increase is estimated to be by around 3% in 100 years. Although the value of the average annual energy in the future did not change significantly, the investigation shows that the monthly wave energy changes are significant, especially in autumn and winter. For evaluating this, at a depth of 29 meters, the energy variations in the study area in Chabahar were extracted, and the values were analyzed. The location of the selected point is shown in Table 1 and Figure 2. Table 3 shows the average value of the wave energy in each month. Table 4 illustrates the exploitable energy percentage. The comparison between energy and exploitable energy in the past and future has been presented in Figure 7.

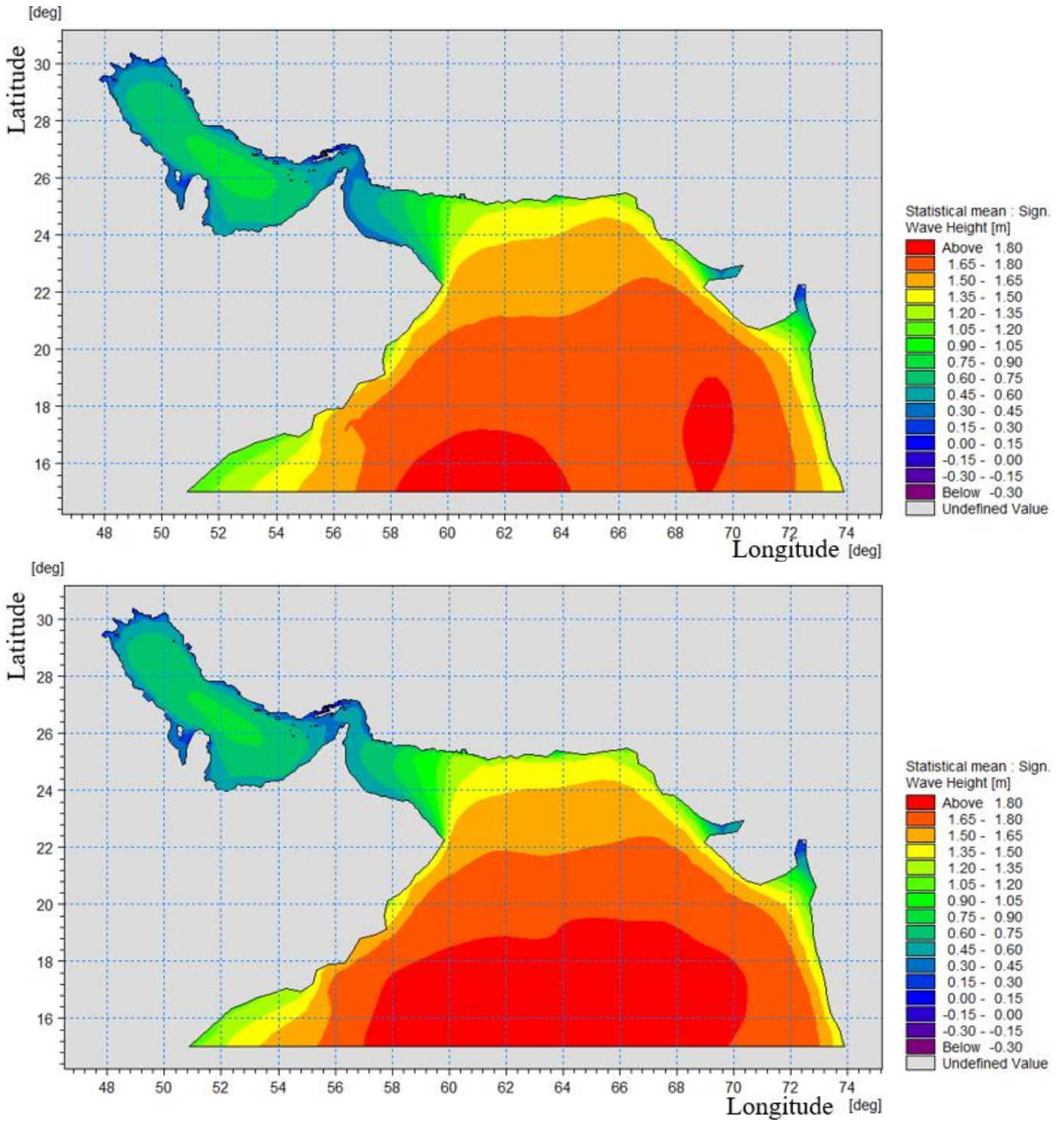


Figure 5. The statistical average of the significant wave height 1991-2000 (up) and 2091-2100 (down)

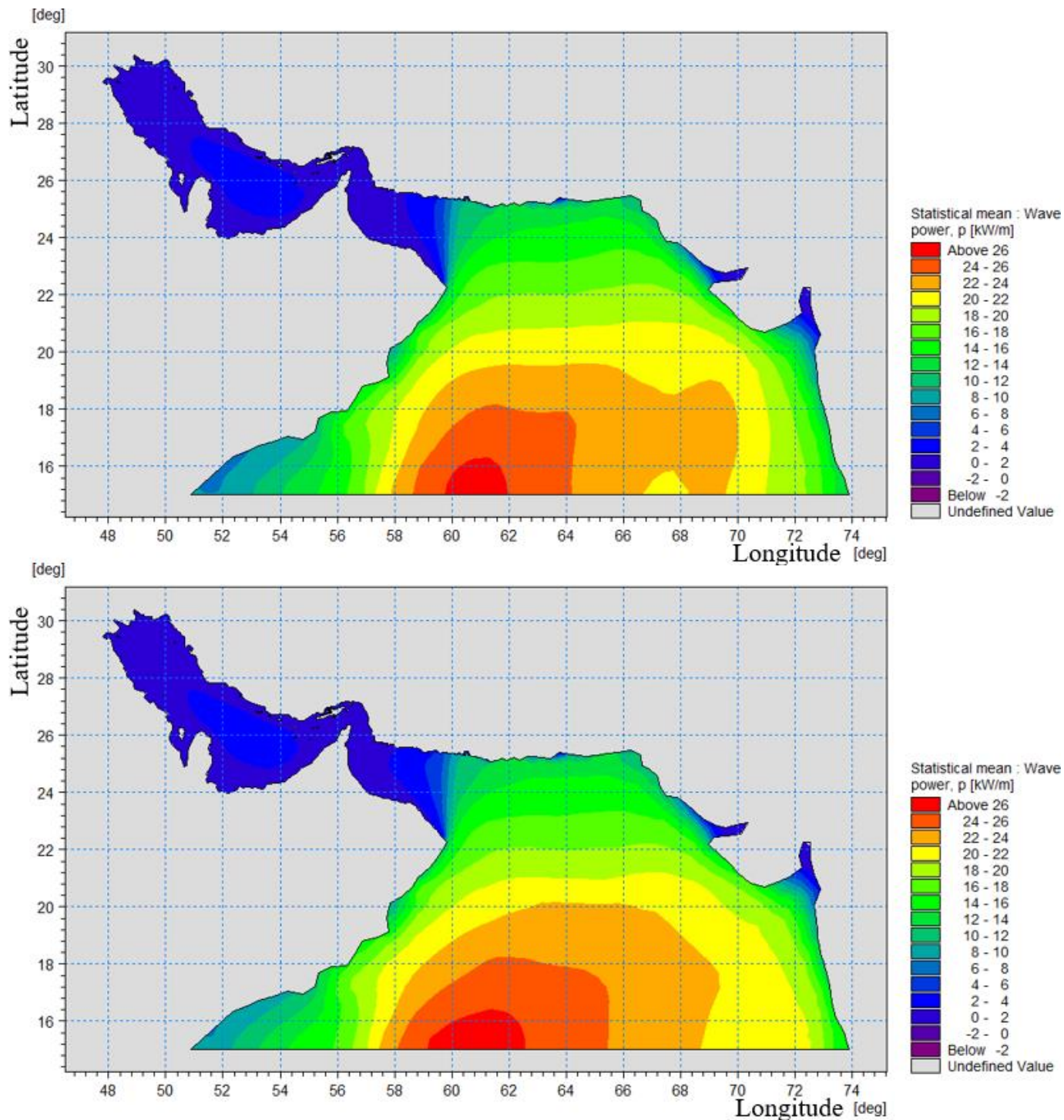


Figure 6. Statistical average of the wave power 1991-2000 (up) and 2091-2100 (down)

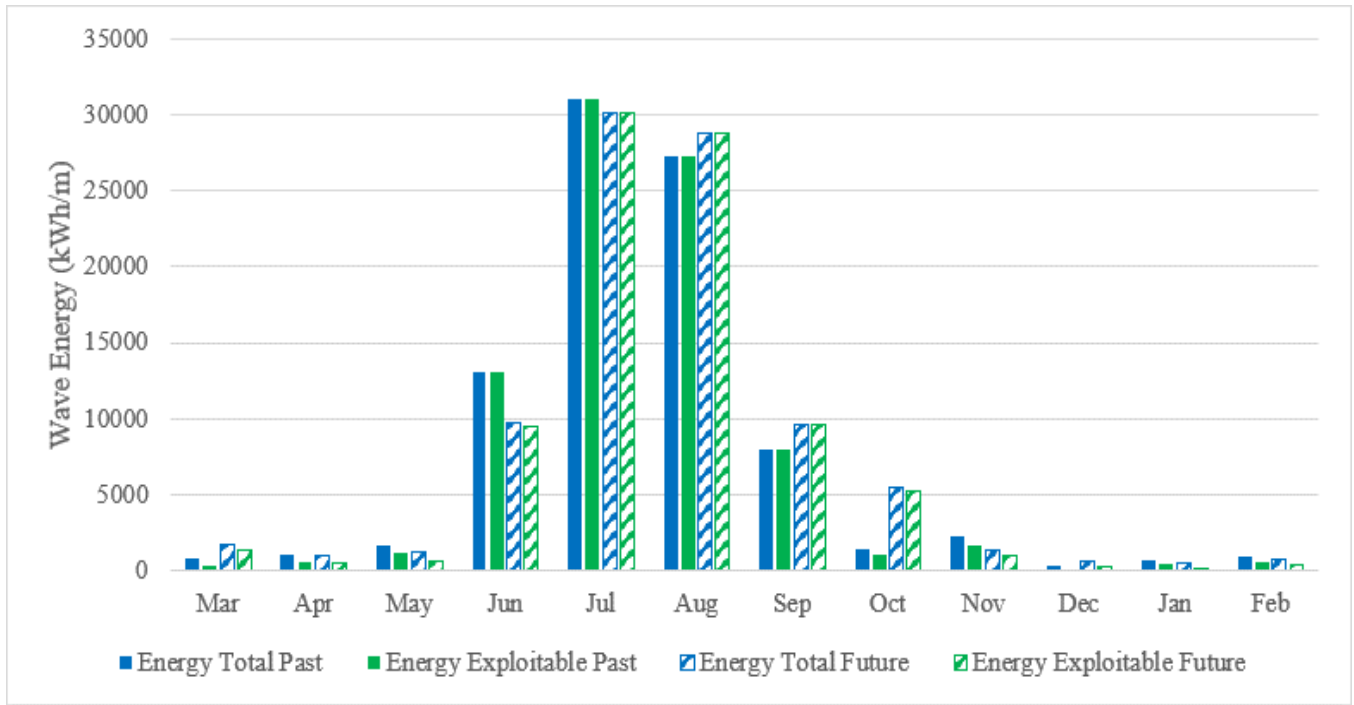


Figure 7. The average value of the wave energy in different months in the future (2091-2100) and past (1991-2000)

Table 3. The average value of the wave energy and power in the past (1991-2000) and future (2091-2100)

		Period	Mar	Apr	May	Jun	Jul	Aug	Sep	Oct	Nov	Dec	Jan	Feb	year
P <sub>ave</sub> kW/m	Total	Past	1.01	1.52	2.16	18.11	41.69	36.69	11.01	1.97	3.11	0.41	0.92	1.31	10.10
		Future	2.33	1.36	1.65	13.55	40.53	38.71	13.37	7.44	1.84	0.79	0.67	1.14	10.40
	Exploitable	Past	3.38	3.94	3.70	18.11	41.69	36.69	11.01	2.74	10.49	0.00	4.28	6.45	20.10
		Future	7.91	3.59	2.79	16.72	40.53	38.71	13.37	8.97	5.36	0.00	2.71	3.60	20.21
Energy kWh/m	Total	Past	766	1093	1610	13041	31019	27300	7925	1466	2240	305	675	883	88323
		Future	1761	978	1225	9754	30157	28801	9624	5535	1322	584	493	767	91002
	Exploitable	Past	284	630	1214	13041	31019	27300	7925	1065	1699	0	398	600	85174
		Future	1376	485	616	9513	30157	28801	9624	5294	982	252	98	442	87641

Table 4. Exploitability of wave energy

		Period	Mar	Apr	May	Jun	Jul	Aug	Sep	Oct	Nov	Dec	Jan	Feb	year
Exploitable time %	Past	11%	22%	44%	100%	100%	100%	100%	52%	23%	0%	13%	14%	48%	
	Future	23%	19%	30%	79%	100%	100%	100%	79%	25%	13%	5%	18%	49%	
Exploitation	Past	37%	58%	75%	100%	100%	100%	100%	73%	76%	0%	59%	68%	96%	
	Future	78%	50%	50%	98%	100%	100%	100%	96%	74%	43%	20%	58%	96%	

Obviously in the graph, the wave energy is higher in the summer. It is due to the Monsoon wind regime and waves propagated by it. These waves come from the southeast and the Indian Ocean [17]. As can be seen with a glance at the results, the amount of wave energy in the Chabahar area is much higher than other areas of the country's southern coasts, such as the coasts of the Persian Gulf. This is generally due to the presence of monsoon winds and their intensity and the pattern of these winds. The coincidence of this phenomenon with the time of need for energy in southern part of country based on high consumption of electric air-conditions can justify the extraction of energy from waves. Meanwhile, in general, the uniformity of energy throughout the year is not very suitable.

The average wave power and energy will increase by about 3%. The average power is about 10 kW/m. In July, however, the value of power exceeds 40 kW/m. July and August have the most powerful waves. Generally, results from the future wave simulation indicate that the procedure will repeat and this time of year will remain the most powerful month.

The most increase occurs in autumn. In this season, the value is expected to increase by about 2.24 kW/m, which equals 27% of its past period. Wave power is reduced by 2.27 kW/m during winter months. This value is significant regarding that the total wave energy in winter is 5.4 kW/m and shows a 42% reduction. In the two most powerful months (July and August) we have about a 1% increase in the power. July and August are first two powerful months and they also remain the most powerful months in future. In July we will have about 3% decrease in the wave energy while in August wave energy will increase about 5%. Totally we can say there is about 1% increase in wave energy in these two months.

Analyzing the values of the monthly average shows that the monthly energy changes, vary between a 4229 kWh/m increase in October to a 3528 kWh/m reduction in June. Similarly, analyzing the percentage of changes shows that October has also had the largest increase in percentage terms, equal to 277%, and November had the largest reduction, equivalent to 41% or 717 kWh/m.

## 5. Conclusions

The results of this research are summarized below:

1. In an intermediate climate change scenario, the average annual wave power in the area of Chabahar will increase by about 3 percent and reaches 10.4 kW/m in the decade ending in 2100 compared to a similar period in the previous century.
2. Similar to the past (1991-2000), summer will be the most energetic season in the future (2091-2100). During autumn, wave energy increases the most. The value of power increase is 2.24 kW/m on average in autumn, which shows a 27% increase compared to the past period. due to winter with a reduction of 42%, the average wave power reaches to 3.09 kW/m.

3. In the last decade of the century, October is the month with the greatest increase in energy. In this month the value of energy increasing is 4229 kW/m, which is equivalent to a 277% increase. June and November have the lowest and highest energy reduction percentage, respectively.

## 8. References

- [1] Şan M, Akpınar A, Bingölbali B, Kankal M. Geospatial multi-criteria evaluation of wave energy exploitation in a semi-enclosed sea. *Energy* 2021. <https://doi.org/10.1016/j.energy.2020.118997>.
- [2] Portilla J, Sosa J, Cavaleri L. Wave energy resources: Wave climate and exploitation. *Renewable Energy* 2013. <https://doi.org/10.1016/j.renene.2013.02.032>.
- [3] Alizadeh MJ, Alinejad-Tabrizi T, Kavianpour MR, Shamshirband S. Projection of spatiotemporal variability of wave power in the Persian Gulf by the end of 21st century: GCM and CORDEX ensemble. *Journal of Cleaner Production* 2020. <https://doi.org/10.1016/j.jclepro.2020.120400>.
- [4] Sierra JP, Casas-Prat M, Campins E. Impact of climate change on wave energy resource: The case of Menorca (Spain). *Renewable Energy* 2017. <https://doi.org/10.1016/j.renene.2016.08.060>.
- [5] Rusu L. Evaluation of the near future wave energy resources in the Black Sea under two climate scenarios. *Renewable Energy* 2019. <https://doi.org/10.1016/j.renene.2019.04.092>.
- [6] Cuttler MVW, Hansen JE, Lowe RJ. Seasonal and interannual variability of the wave climate at a wave energy hotspot off the southwestern coast of Australia. *Renewable Energy* 2020. <https://doi.org/10.1016/j.renene.2019.08.058>.
- [7] Iribarren D, Martín-Gamboa M, Navas-Anguita Z, García-Gusano D, Dufour J. Influence of climate change externalities on the sustainability-oriented prioritisation of prospective energy scenarios. *Energy* 2020. <https://doi.org/10.1016/j.energy.2020.117179>.
- [8] Martínez A, Iglesias G. Wind resource evolution in Europe under different scenarios of climate change characterised by the novel Shared Socioeconomic Pathways. *Energy Conversion and Management* 2021;234:113961. <https://doi.org/https://doi.org/10.1016/j.enconman.2021.113961>.
- [9] Martínez A, Iglesias G. Climate change impacts on wind energy resources in North America based on the CMIP6 projections. *Science of The Total Environment* 2022;806:150580. <https://doi.org/https://doi.org/10.1016/j.scitotenv.2021.150580>.
- [10] Pourali M, Kavianpour MR, Kamranzad B, Alizadeh MJ. Future variability of wave energy in the Gulf of Oman using a high resolution CMIP6 climate model. *Energy* 2023;262:125552.

<https://doi.org/https://doi.org/10.1016/j.energy.2022.125552>.

[11] Saket A, Etemad-Shahidi A. Wave energy potential along the northern coasts of the Gulf of Oman, Iran. *Renewable Energy* 2012.

<https://doi.org/10.1016/j.renene.2011.09.024>.

[12] Kamranzad B, Chegini V, Etemad-Shahidi A. Temporal-spatial variation of wave energy and nearshore hotspots in the Gulf of Oman based on locally generated wind waves. *Renewable Energy* 2016. <https://doi.org/10.1016/j.renene.2016.03.084>.

[13] Kamranzad B, Hadadpour S. A multi-criteria approach for selection of wave energy converter/location. *Energy* 2020;204:117924.

<https://doi.org/https://doi.org/10.1016/j.energy.2020.117924>.

[14] DHI. MIKE 21 SW - Spectral Wave Model: Scientific Documentation. DHI Water and Environment 2014.

[15] Tucker MJ, Pitt EG. *Waves in ocean engineering* 2001.

[16] (U.S.) RE and AUP. Technology white paper on wave energy potential on the U.S. Outer Continental Shelf. 2006.

[17] Sanil Kumar V, Singh J, Pednekar P, Gowthaman R. Waves in the nearshore waters of northern Arabian Sea during the summer monsoon. *Ocean Engineering* 2011. <https://doi.org/10.1016/j.oceaneng.2010.11.009>.